

CONF-970591--2

INVESTIGATION OF A NON-CONTACT STRAIN MEASUREMENT TECHNIQUE

by

L. J. Talarico  
and  
B. Damiano

Oak Ridge National Laboratory  
Oak Ridge, Tennessee

RECEIVED

MAR 18 1997

OSTI

Manuscript submitted to the  
International Conference on Maintenance and Reliability  
MARCON 97  
May 20-22, 1997  
Knoxville, Tennessee

The submitted manuscript has been authored by a contractor of the U.S. Government under contract AC05-96OR22464. Accordingly, the U.S. Government retains a nonexclusive, royalty-free license to publish or reproduce the published form of this contribution, or allow others to do so, for U. S. Government purposes.

Research sponsored by the Laboratory Directed Research Program of Oak Ridge National Laboratory.

DISTRIBUTION OF THIS DOCUMENT IS UNLIMITED



MASTER

This research was performed at OAK RIDGE NATIONAL LABORATORY, managed by LOCKHEED MARTIN ENERGY RESEARCH CORP. for the U.S. DEPARTMENT OF ENERGY under contract number DE-AC05-96OR22464.

## DISCLAIMER

This report was prepared as an account of work sponsored by an agency of the United States Government. Neither the United States Government nor any agency thereof, nor any of their employees, make any warranty, express or implied, or assumes any legal liability or responsibility for the accuracy, completeness, or usefulness of any information, apparatus, product, or process disclosed, or represents that its use would not infringe privately owned rights. Reference herein to any specific commercial product, process, or service by trade name, trademark, manufacturer, or otherwise does not necessarily constitute or imply its endorsement, recommendation, or favoring by the United States Government or any agency thereof. The views and opinions of authors expressed herein do not necessarily state or reflect those of the United States Government or any agency thereof.

**DISCLAIMER**

**Portions of this document may be illegible  
in electronic image products. Images are  
produced from the best available original  
document.**

# INVESTIGATION OF A NON-CONTACT STRAIN MEASUREMENT TECHNIQUE

L. J. Talarico and B. Damiano  
Oak Ridge National Laboratory  
Oak Ridge, Tennessee 37831 - 6010

Research sponsored by the Laboratory Directed Research Program of Oak Ridge National Laboratory

## 1. ABSTRACT

The goal of this project was to investigate the feasibility of a new non-contact technique for directly and continuously monitoring peak strain in rotating components. The technique utilizes the unique strain-sensitive magnetic material properties of Transformation Induced Plasticity (TRIP) steel alloys to measure strain. These alloys are weakly magnetic when unstrained but become strongly ferromagnetic after mechanical deformation. A computer study was performed to determine whether the strain-induced change in the magnetic material properties of a TRIP steel gage bonded to a rotating component would cause significant perturbations in the magnetic flux of a stationary electromagnet. The effects of strain level, distance between the rotating component and the stationary electromagnet, and motion-induced eddy currents on flux perturbation magnitude were investigated.

The calculated results indicate that a TRIP steel strain sensing element can cause a significant perturbation in the magnetic flux of a stationary electromagnet. The magnetic flux perturbation magnitude was found to be inversely proportional to the distance between the magnet face and the TRIP steel element and directly proportional to the TRIP steel strain level. The effect of motion-induced eddy currents on the magnetic flux was found to be negligible. It appears that the technique can be successfully applied to measure peak strain in rotating components, however, the sensitivity of the magnetic flux perturbation magnitude to the distance between the strain sensing element and the electromagnet may require making an independent proximity measurement.

## 2. INTRODUCTION

The project described in this report investigated a new technique for directly and continuously monitoring peak strain in rotating components. Current techniques for monitoring the structural condition of rotating components use an indirect indication of structural degradation, such as abnormal noise due to excessive vibration, or use a direct indication obtained by examining the rotating component during shutdown. Although failure of rotating components is relatively rare due to conservative design and intense maintenance and inspection programs, occasional failures can have severe economic or safety consequences. An example of steam turbine blade failure at the Fermi-2 nuclear plant on December 25, 1993 is estimated to have cost Detroit Edison in excess of \$35 million.<sup>1</sup> Continuous monitoring of rotating components could possibly eliminate some of the currently performed maintenance and inspection procedures, while increasing the reliability of these components.

The technique combines the use of a TRIP (Transformation Induced Plasticity)<sup>2</sup> steel strain sensing element attached to the rotating component, a stationary magnetic coil to provide a magnetic field, and a stationary magnetic field sensor to measure changes in the magnetic field caused by magnetic property changes in the strain sensing element. This technique uses the metastable structure of TRIP steel to measure maximum strain. TRIP steels are initially in a metastable austenitic face-centered cubic phase. When subjected to

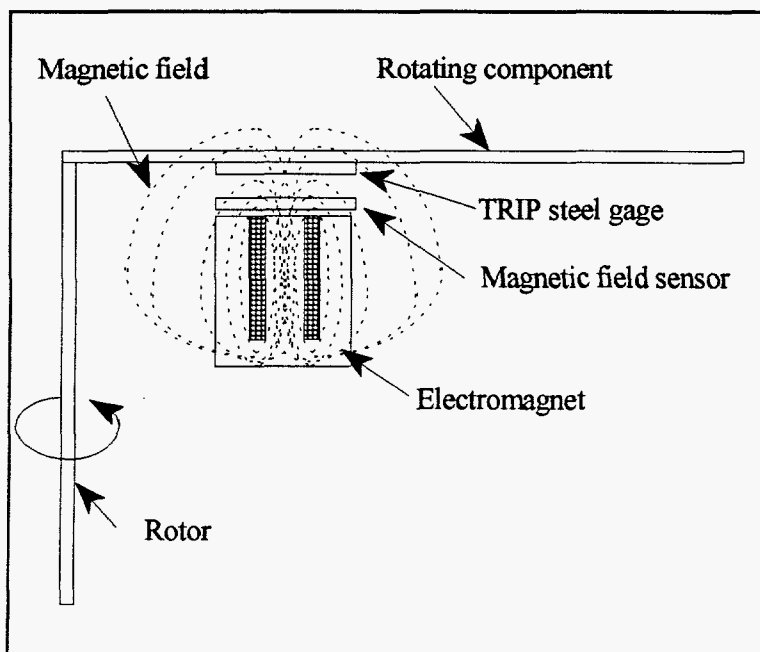
deformation, the crystal structure changes to a martensitic body-centered tetragonal phase, with the amount of material undergoing the phase change being proportional to the peak strain.<sup>2</sup> The martensitic phase is ferromagnetic while the austenitic phase is paramagnetic; thus, the magnetic properties can be used to determine the prior peak strain a part has experienced. TRIP steel sensors have been applied to measure strain in stationary components such as bridge members and for structural mining applications.<sup>3</sup> The innovative aspects of this project are the extension of this application to rotating components and the use of TRIP steel sensors to perform continuous strain monitoring.

The TRIP steel sensing elements are used to indicate high strain levels in rotating components in the following way (Figure 1):

- 1) Attach the TRIP steel strain sensing element to the rotating component at the location where peak strains or failure are known or are predicted to occur. The sensing element may be a strip located inside the rotating component or a foil bonded to the surface.
- 2) Mount a stationary magnetic coil so that the magnetic field produced will interact with the TRIP steel strain sensing element during part of the component's rotation.
- 3) Mount a stationary magnetic field sensor, such as a Hall effect probe, to measure the coil's magnetic field strength.

Initially, with the strain sensing elements unstrained, the magnetic field sensor should detect little or no change in the coil's magnetic field when the strain sensing element is within the region occupied by the magnetic field. As the strain sensing elements deform, making the strain sensing element more ferromagnetic, it is anticipated that magnetic field perturbations will occur when the strain sensing element passes through the magnetic field. These perturbations should be measurable for sufficiently large strains. The magnetic field fluctuations can be related to the amount of ferromagnetic martensitic material in the

strain sensing element and thus to the amount of strain experienced by the rotating component.



The feasibility of the technique was investigated by applying the ElectroMagnetic Analysis System (EMAS) computer code, developed and distributed by the MacNeal-Schwendler Corporation, to calculate the magnetic fields near the magnetic coil.<sup>4</sup> The effect on the magnetic field caused by variations in the magnetic properties of the TRIP steel strain sensor, the gap between the coil and the strain sensor, and the rotation speed were examined. A description of the EMAS model and the parametric study is presented in Section 3. Section 4 presents the calculation results, and conclusions are presented in Section 5.

Figure 1. A typical application of a TRIP steel sensor to measure strain in a rotating component.

### 3. FINITE ELEMENT MODEL AND PARAMETRIC STUDY DESCRIPTION

The finite element models used to investigate the magnetic flux perturbations caused by the strain-induced phase transformation in the TRIP steel strain sensing element are described in this section. Axisymmetric, two-dimensional static, and two-dimensional transient models were used in the analysis. The axisymmetric models were used to calculate the three-dimensional magnetic flux density when the TRIP steel strain sensor (which was modeled as a 0.635 mm thick disk) was centered over the magnet. These results were used as the base analysis results. The three-dimensional magnetic flux and the two-dimensional magnetic flux are expected to be affected in quantitatively similar ways by motion-induced eddy currents. Thus, by comparing the calculated magnetic flux densities for the two-dimensional static and two-dimensional transient models, the effect on the three-dimensional magnetic flux could be estimated. A three-dimensional transient model could not be run to verify the validity of this assumption because of a lack of computer resources.

The finite element model is shown in Figure 2. The model was created by meshing a cross section of the three-dimensional geometrical model of the system. The model is composed of an electrical steel armature, a coil, the TRIP steel disk, and a cylindrical volume of surrounding air. The magnetic flux was constrained to be tangent to the outer surface of the air region and a steady-state excitation was applied to the coil regions to account for current flow through the coil. The coil excitation equals the total current flowing out of the cross-sectional area of the coil, which is calculated by multiplying the number of coil turns by the coil current. The value used for the coil excitation,  $C_{cs}$ , is given by

$$C_{cs} = \frac{0.785 A_c A_{max}}{A_w}, \quad (1)$$

where  $A_c$  is the total coil cross-sectional area,  
 $A_w$  is the cross-sectional area of the wire,  
 $A_{max}$  is the maximum current capacity of the wire, and  
0.785 is the coil space factor for round wires.<sup>5</sup>

Assuming AWG #17 wire (diameter = 1.23 mm,  $A_{max} = 2$  amperes), the maximum value for  $C_{cs}$  is 700 amperes. A value of 650 amperes was used in the analysis to stay within the maximum coil excitation.

Additional structural constraints and initial conditions were needed for the transient models. All nodes were constrained to be fixed in the  $x$  and  $z$  directions. The rotation of all nodes in the three coordinate directions was also constrained. All nodes except those on the TRIP steel disk and nodes comprising the elements of air surrounding the TRIP steel disk were also constrained in the  $y$  direction. This combination of constraints allowed the TRIP steel disk to move in the  $y$  direction and for the air elements surrounding the disk to deform as a result of the motion. An initial velocity and an initial displacement equal to the distance the disk would move over the analysis time was specified for the nodes comprising the TRIP steel disk. These initial conditions resulted in the centers of the disk and the magnet coinciding during the final time step. The magnetic flux density of the corresponding magnetostatic case was used as the electromagnetic initial condition.

Quadratic quadrilateral elements were used in the axisymmetric models and linear quadrilateral elements were used in the two-dimensional static and transient models. Quadratic elements are preferable to linear elements because they give more accurate results for the same number of elements. However, limitations inherent in the EMAS code prevented quadratic elements from being used in the transient models; because the two-dimensional transient model used the two-dimensional static model results as initial conditions, linear elements were also used in the two-dimensional static models. The regions with the greatest mesh density,

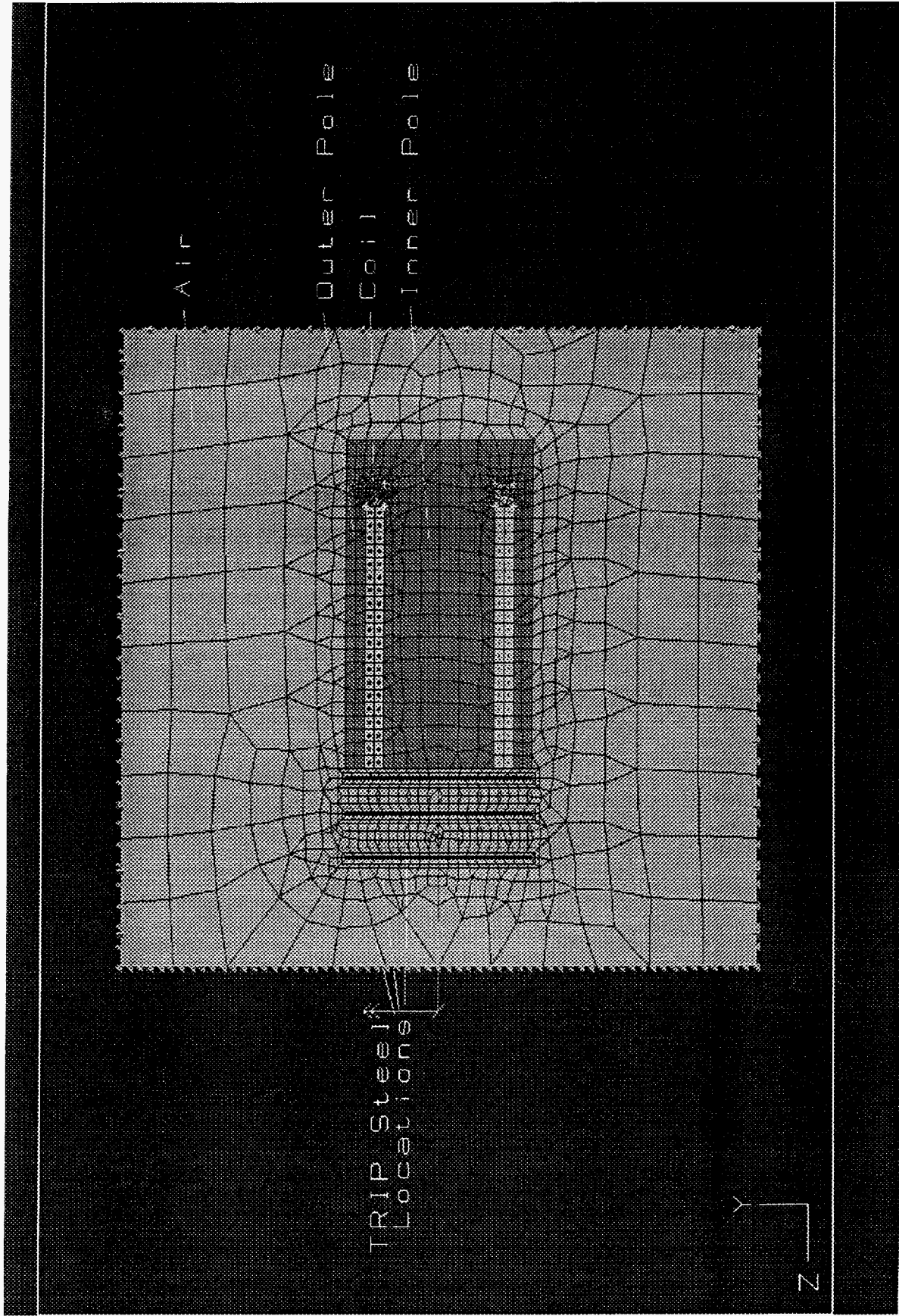


Figure 2. The finite element model.

the TRIP steel disk regions and the bottom of the coil region, were meshed first. The steel armature was meshed next and the air region was meshed last. After placing the electromagnetic boundary conditions and excitations on the model, an input file for EMAS was created.

If an input file for a transient model was being created, the initial EMAS input file was modified to include the structural constraints, the transient calculation control information (start time, end time, and time step) and the initial electromagnetic and structural conditions. The resulting file was then ready to be used to calculate a coupled electromagnetic/structural transient solution.

The parametric study examined the effects of air gap, TRIP steel element magnetic properties, and TRIP steel disk speed on the magnetic flux density. Air gaps of 2.54 mm, 12.7 mm, and 25.4 mm were used in this study. The TRIP steel magnetic properties, which were provided for 100% strained material, were modified to simulate the properties of lower strain. The flux density ( $B$ ) values for reduced strain cases were calculated by multiplying the 100% strained TRIP steel  $B$  values by the strain level for low values of magnetomotive force ( $H$ ). At large values of  $H$  (i.e., for values of  $H$  beyond the "knee" of the  $B$ - $H$  curve), the  $B$ - $H$  curves were given a slope of  $\mu_0$ . This practice makes the modified  $B$ - $H$  curves conform to those provided by the MacNeal-Schwendler Corporation and results in more rapid convergence of the numerical solution. However, solutions containing flux densities greater than that corresponding to the "knee" of  $B$ - $H$  curves modified in this way must be discarded. The resulting  $B$ - $H$  curves are shown in Figure 3. Strain levels of 10, 25, 50, 75, and 100 percent were used in the analysis. In the transient cases, TRIP steel disk velocities of 2.54 m/sec, 12.7 m/s, and 25.4 m/s were used.

The axisymmetric magnetic flux calculated for the 100% strained TRIP steel disk located at 2.54 mm is shown in Figure 4. The results show the magnetic flux confined primarily in the electrical steel armature, with flux concentrations at the corners of the coil slot and in the TRIP steel disk between the inner and outer magnet poles. The difference in the axisymmetric magnetic flux densities for a case with no TRIP steel and a case with 100% strained TRIP steel located at 2.54 mm is shown in Figure 5. Figure 5 shows the spatial perturbation in magnetic flux caused by the TRIP steel disk. These results show that the optimum location for the flux density instrumentation is on the front face of the magnet because this location experiences a larger flux perturbation than any other portion of the air region. Therefore, the magnetic flux density averaged over the face of the magnet inside the coil (i.e., the inner pole),  $\bar{B}$ , will be used as the measure of magnetic flux when presenting the analysis results.

#### 4. CALCULATION RESULTS

The results of the parametric study are presented in this section. The results for the axisymmetric static cases are presented first, followed by the results for the two-dimensional coupled electromagnetic/structural transient cases.

##### 4.1 Axisymmetric Magnetostatic Results

The axisymmetric magnetic flux density averaged over the inner pole face,  $\bar{B}$ , for TRIP steel disk strains ranging from 0 to 100% and air gaps of 2.54 mm, 12.7 mm, and 25.4 mm is shown in Figure 6 and listed in Table 1. The results show that  $\bar{B}$  is very sensitive to air gap and somewhat sensitive to TRIP steel strain level. Neglecting the effects of motion-induced eddy currents (which will be examined in the next section), the difference between each case and the all air case is the maximum perturbation magnitude one would measure for the TRIP steel disk passing the stationary magnetic coil.



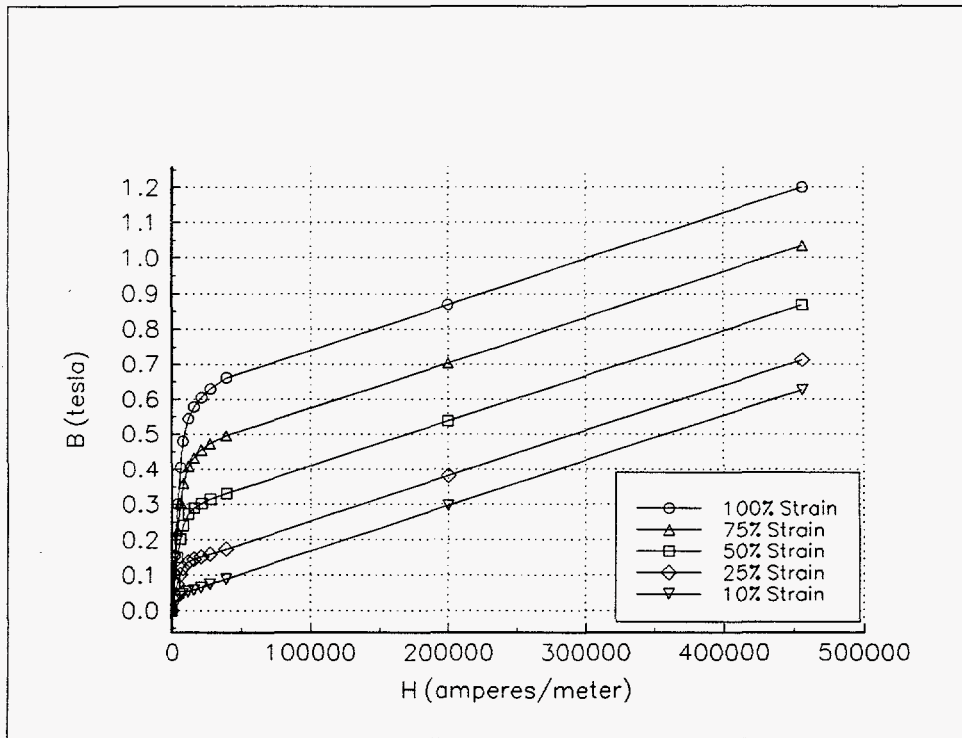


**Figure 3. B-H curves used in the analysis for TRIP steel .**

**Table 1  
Effect of TRIP Steel Strain and Air Gap on Average Inner Pole Flux Density**

Strain Level (%)	B for 2.54 mm air gap (tesla)	B for 12.7 mm air gap (tesla)	B for 25.4 mm air gap (tesla)
0	0.0423	0.0423	0.0423
10	0.0432	0.0424	0.0423
25	0.0452	0.0426	0.0424
50	0.0479	0.0428	0.0424
75	0.0504	0.0429	0.0424
100	0.0525	0.0430	0.0425

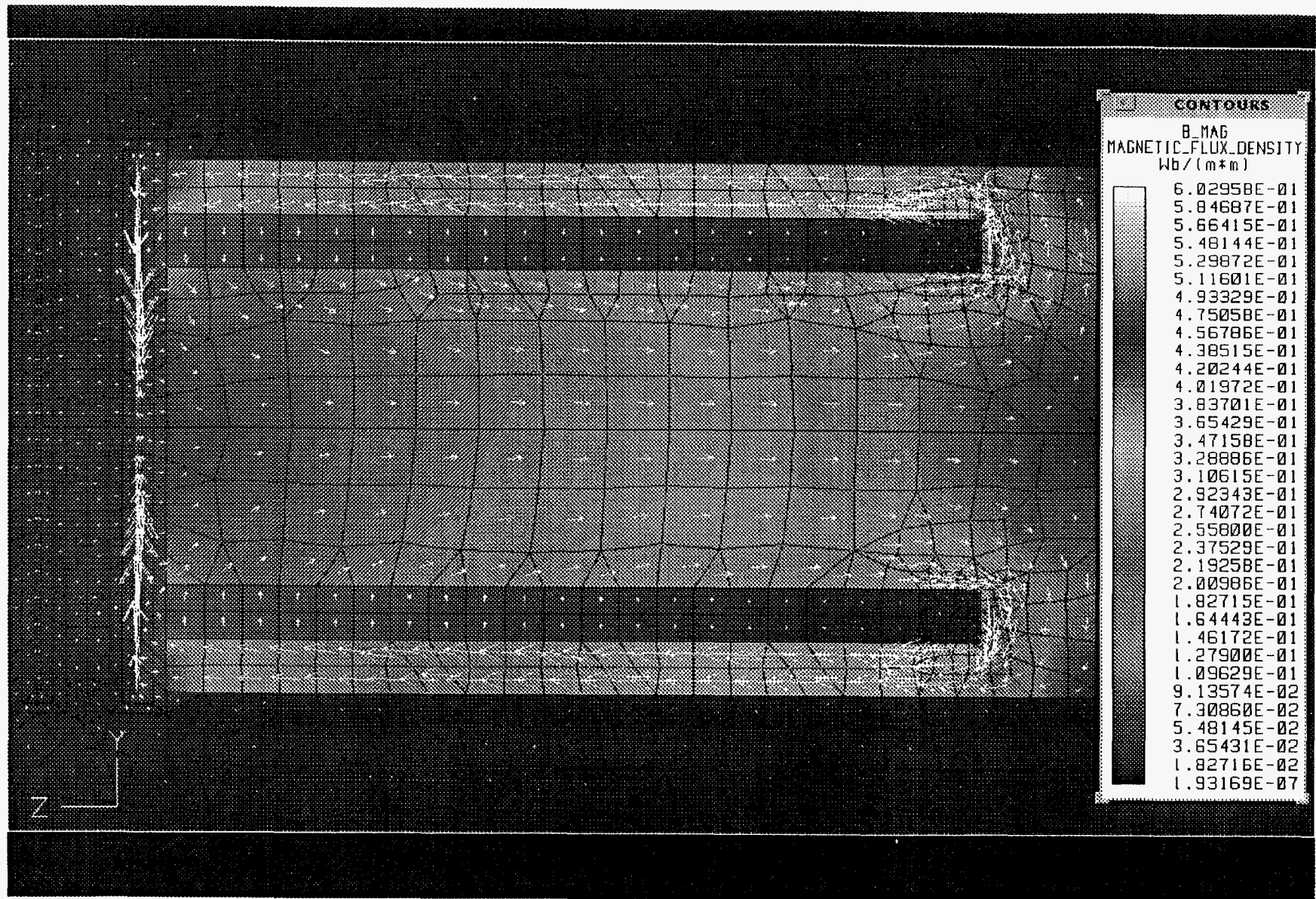


Figure 4. Flux density for 100% strained TRIP steel with a 2.54 mm air gap.

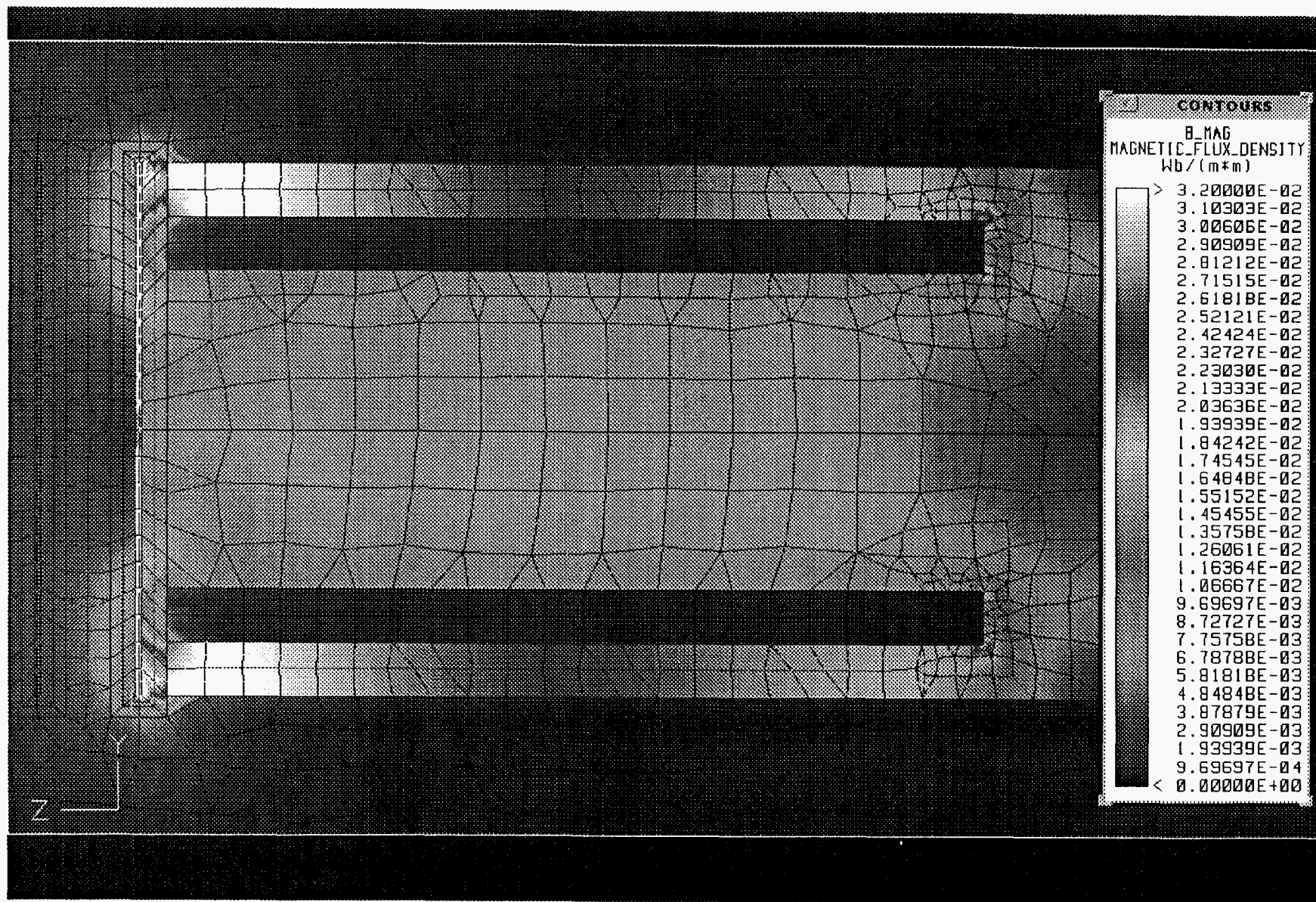
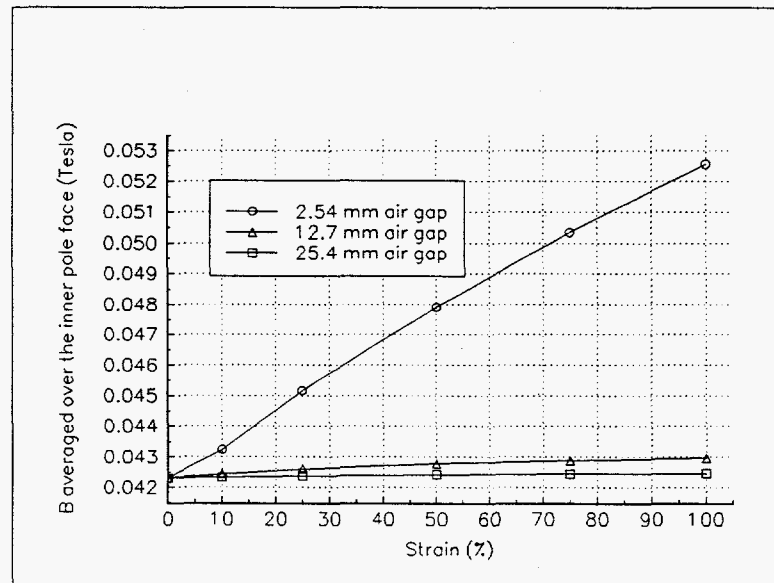


Figure 5. Magnetic flux perturbation caused by the presence of 100% strained TRIP steel with a 2.54 mm air gap.

## 4.2 Two-Dimensional Magnetostatic and Nonlinear Transient Results

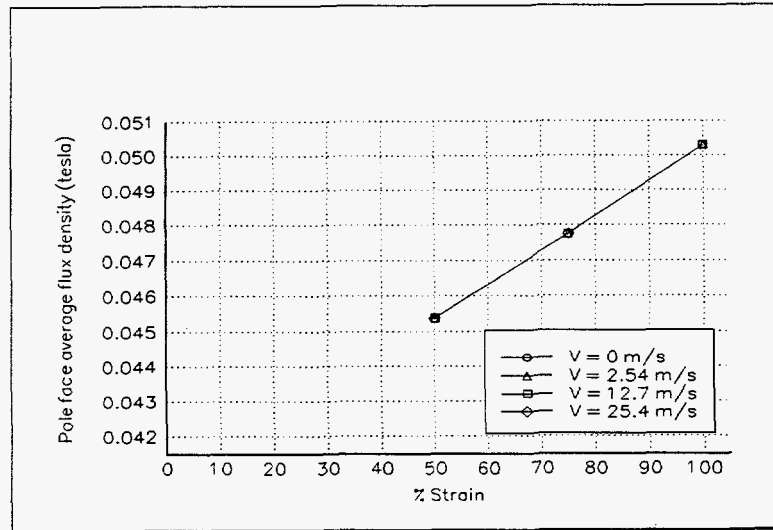
The two-dimensional model was used to examine the effects of motion-induced eddy currents on the magnetic flux density. The transient cases were given an initial velocity and an initial displacement such that during the final time step the TRIP steel elements were centered over the magnet. The calculated values of  $B$  for initial velocities of 2.54 m/s, 12.7 m/s, and 25.4 m/s are shown for a 2.54 mm air gap in Figure 7, for a 12.7 mm air gap in Figure 8, and for a 25.4 mm air gap in Figure 9. For each air gap, the effect of the initial velocity is negligible; the curves showing the average pole face flux density for different velocities are virtually indistinguishable from each other. This similarity is believed to be caused by the small thickness of the TRIP steel disk, by the magnetic flux density not being particularly large in the TRIP steel disk, and by the small rate of change in magnetic flux density over the range of motion examined in this study (i.e., near the centerline of the magnet).

Figure 10 shows the two-dimensional, zero velocity results calculated for the three different air gaps. Comparison of Figures 6 and 10 show qualitatively similar behavior; the flux density is highly dependent on the air gap thickness and somewhat less dependent on the TRIP steel strain level. The main conclusion that can be reached from the transient case results is that because the effect of motion-induced eddy currents is negligible, the axisymmetric results shown in Figure 6 give an accurate indication of the magnetic flux perturbations caused by the presence of the TRIP steel disk.



**Figure 6. Magnetic flux density averaged over the inner pole face for strain levels ranging from 0% to 100% and air gaps of 2.54 mm, 12.7 mm, and 25.4 mm.**





**Figure 7. Magnetic flux density averaged over the pole face for strain levels ranging from 50% to 100%, TRIP steel disk velocities of 0 m/s, 2.54 m/s, 12.7 m/s, and 25.4 m/s and an air gap of 2.54 mm. The 10% and 25% cases are not shown because these cases failed to converge.**

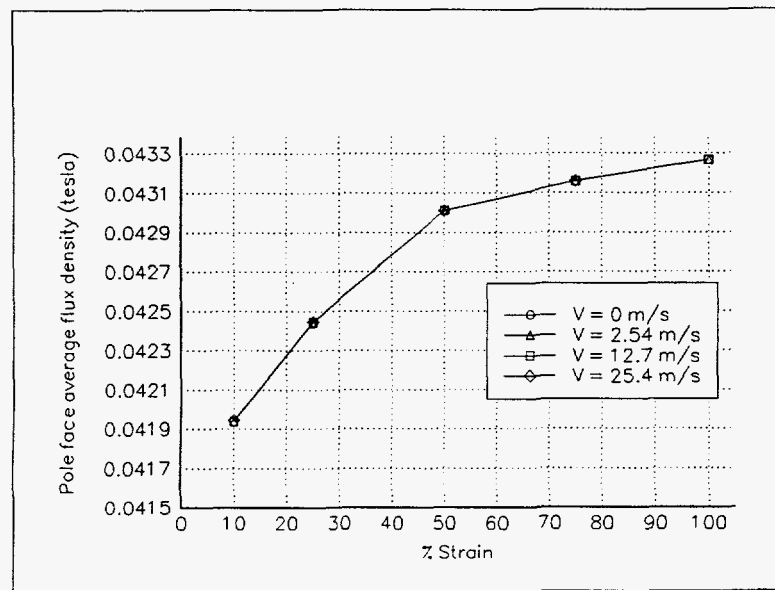


**Figure 8. Magnetic flux density averaged over the pole face for strain levels ranging from 10% to 100%, TRIP steel disk velocities of 0 m/s, 2.54 m/s, 12.7 m/s, and 25.4 m/s and an air gap of 12.7 mm.**

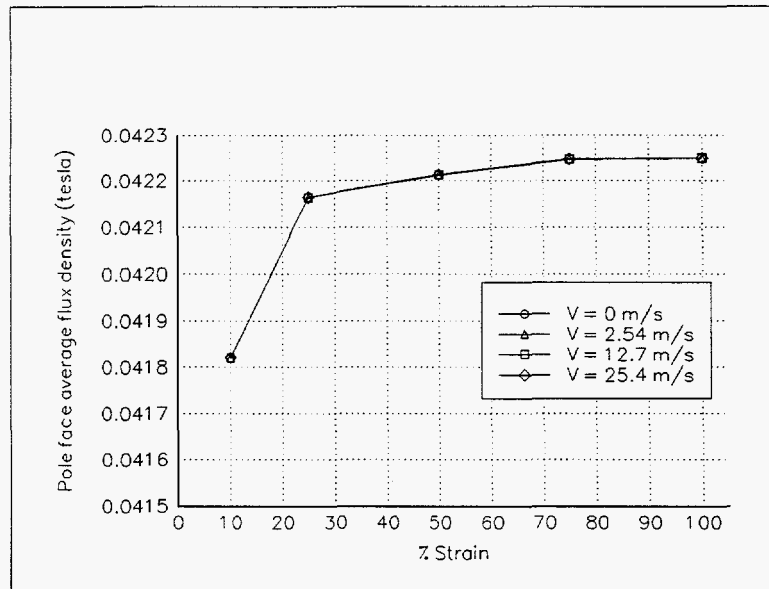


**Figure 9. Magnetic flux density averaged over the pole face for strain levels ranging from 10% to 100%, TRIP steel disk velocities of 0 m/s, 2.54 m/s, 12.7 m/s, and 25.4 m/s and an air gap of 25.4 mm.**

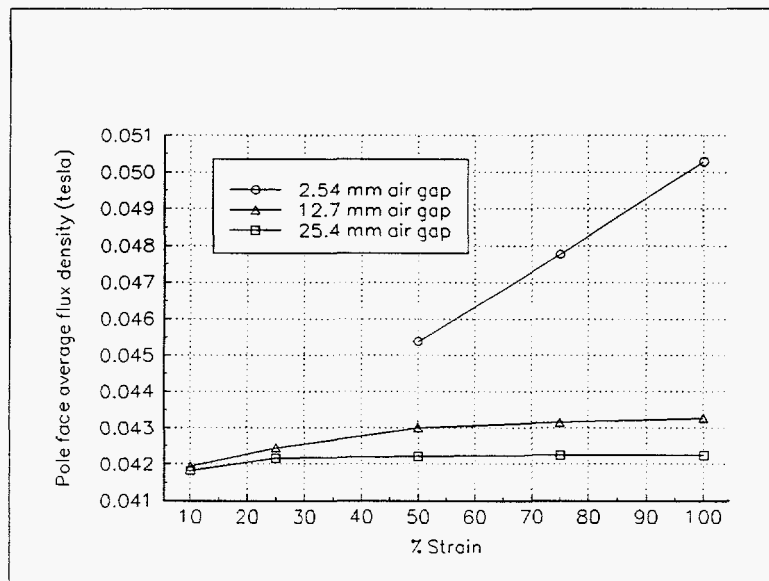


**Figure 10. Magnetic flux density averaged over the pole face for strain levels ranging from 10% to 100% and air gaps of 2.54 mm, 12.7 mm, and 25.4 mm.**

## 5. CONCLUSIONS

The calculated results indicate that the strain-induced change in TRIP steel disk properties can cause significant flux density perturbations as the disk passes the magnet face. The perturbation magnitude is affected by the air gap thickness and by the magnetic material properties of the TRIP steel disk; decreasing the air gap results in a greater sensitivity of the magnetic flux to TRIP steel disk material properties. Finally, it appears that the effect of motion-induced eddy currents on the magnetic flux density perturbations is negligible.

The calculated results suggest that strains in rotating components can be measured by using a TRIP steel gage bonded to the rotating part. The measurement will be most accurate for small air gaps, (approximately 6.4 mm or less) because the measurement sensitivity increases rapidly as the air gap thickness decreases. Thus, the measurement could be made most easily on systems that allow small air gap thicknesses. Because of the rapid change in measurement sensitivity with air gap thickness, a system that can experience significant air gap thickness fluctuations will require an independent proximity measurement.

The negligible effect of motion-induced eddy currents on the flux density perturbations allows future analytical studies to be performed using simple axisymmetric or two dimensional models. Thus, any future design or analysis work can be expected to be performed faster and may even be performed using smaller, less sophisticated analysis codes.

## 6. REFERENCES

1. Nuclear News, Volume 37, Number 7, page 21, May 1994.
2. V. F. Zackay, E. R. Parker, D. Fahr, and R. Busch, "The Enhancement of Ductility in High-Strength Steels", Transactions of the American Society of Metals, Vol. 60, pp. 252-259, 1967.
3. "A Damage Monitoring Technology for Safety Assessment of Structural Materials", Report # 46-94, Strain Monitor Systems, Inc., San Diego, CA 1994.
4. J. R. Brauer, B. E. MacNeal, and J. C. Neuner, MSC/EMAS Users Manual, Version 3, The MacNeal-Schwendler Corporation, 815 Colorado Blvd, Los Angeles, CA. 90041, 1994.
5. Mark's Standard Handbook for Mechanical Engineers, Eighth Edition, McGraw Hill Book Company, New York, 1978.